SOLUTION OF COUPLED HEAT-TRANSFER PROBLEMS IN FLOW ABOUT BODIES OF DIFFERENT SHAPES

V. I. Zinchenko and E. N. Putyatina UDC 533.526+536.24

Several studies [1-3] have been devoted to the solution of coupled heat-transfer problems. Here we examine nonsteady heat transfer in the supersonic flow of an ideal gas about axisymmetric solids of revolution with values of the determining parameters of the problem corresponding to different flow regimes in the boundary layer. Numerical and analytical solutions for heat flux with a nonisothermal surface are compared in the case of laminar flow in the boundary layer. It is shown that in this case heat flux to the body has a structure which is related to the history of development of the thermal and dynamic boundary layers and to the value of the local surface-temperature derivative. Here, substantial errors may result from the use of standard formulas for the heat-transfer coefficient without allowance for dT_w/ds when the values of dT_w/ds are large and the determination of the temperature field in the body is posed as a separate problem. It should be noted that the effect of a nonisothermal surface temperature on heat flux to a wall in flow about plane bodies was examined in [4, 5].

1. In accordance with [2, 3], characteristics of coupled heat transfer will be sought from the solution of a system of equations describing the change in mean values in the boundary layer [3] and the nonsteady equation of heat conduction in the shell of a body with the corresponding initial and boundary conditions.

With allowance for the Dorodnitsyn–Lees variables for the equations of the gas phase in a natural coordinate system connected with the outside surface of the shell, the system of equations appears as follows in dimensionless variables:

$$\frac{\partial}{\partial\eta}\left(l\frac{\partial^2 f}{\partial\eta^2}\right)+f\frac{\partial^2 f}{\partial\eta^2}+\beta\left[\frac{\Theta}{\Theta_e}-\left(\frac{\partial f}{\partial\eta}\right)^2\right]=\alpha\left(\frac{\partial f}{\partial\eta}\frac{\partial^2 f}{\partial\eta\partial s}-\frac{\partial f}{\partial s}\frac{\partial^2 f}{\partial\eta^2}\right); \tag{1.1}$$

$$\frac{\partial}{\partial\eta}\left(\frac{l}{\mathrm{Pr}}\frac{\partial\Theta}{\eta}\right)+f\frac{\partial\Theta}{\partial\eta}=\beta\gamma\frac{\Theta}{\Theta_e}\frac{\partial f}{\partial\eta}-l\gamma\left(\frac{\partial^2 f}{\partial\eta^2}\right)^2+\alpha\left(\frac{\partial f}{\partial\eta}\frac{\partial\Theta}{\partial s}-\frac{\partial f}{\partial s}\frac{\partial\Theta}{\partial\eta}\right); \tag{1.2}$$

$$\pi_\rho\frac{\partial\Theta_1}{\partial\tau}=\frac{1}{H_1 r}\left[\frac{\partial}{\partial s}\left(\frac{r}{H_1}\pi_1\frac{\partial\Theta_1}{\partial s}\right)+\frac{\partial}{\partial y_1}\left(rH_1\pi_1\frac{\partial\Theta_1}{\partial y_1}\right)\right]. \tag{1.3}$$

The boundary and initial conditions are written in the form

$$\frac{\partial f}{\partial\eta}(\infty,s)=1,\ \Theta(\infty,s)=\Theta_e; \tag{1.4}$$

$$\frac{\partial f}{\partial\eta}(0,s)=0,f(0,s)=0,\tilde{q}_w(0,s)\sqrt{\mathrm{Re}}\mathrm{Pr}_m\frac{\lambda_{e0}}{\lambda_{1*}}-\pi_\sigma\Theta_w^4=\pi_1(\Theta_w)\frac{\partial\Theta_1}{\partial y_1}(\tau,s,0); \tag{1.5}$$

$$\frac{\partial\Theta_1}{\partial y_1}\left(\tau,s,\frac{L}{R_N}\right)=0\quad\text{or}\quad\Theta_1\left(\tau,s,\frac{L}{R_N}\right)=\Theta_{1i}; \tag{1.6}$$

$$s=0,\frac{\partial\Theta_1}{\partial s}=0,\ s=s_0,\ \frac{\partial}{\partial s}\left(\frac{r}{H_1}\pi_1\frac{\partial\Theta_1}{\partial s}\right)=0,\ \Theta_1(0,s,y_1)=\Theta_{1i}. \tag{1.7}$$

Here, s is the dimensionless length of an arc reckoned from the critical point on the external contour of the shell; η and y_1 are directed normal to the external contour on different sides; H_1 and r are the Lamé constants; $\gamma = u_e^2/c_pT_{e0}$,

$$\alpha=2\int_0^s\rho_e\mu_e u_e r_w^2ds/(\rho_e\mu_e u_e r_w^2),\ \beta=\alpha/u_e\cdot du_e/ds,$$

Tomsk. Translated from Zhurnal Prikladnoi Mekhaniki i Tekhnicheskoi Fiziki, No. 2, pp. 85-93, March-April, 1986. Original article submitted December 25, 1984.

 0021-8944/86/2702-0234$12.50 © 1986 Plenum Publishing Corporation

$$\pi_1 = \lambda_1/\lambda_{1*},\ \pi_\rho = \rho_1 c_1/\rho_{1*}c_{1*},\ \pi_\sigma = \varepsilon\sigma T_{e0}^3/\lambda_{1*},$$
$$l = \rho(\mu + \Gamma\mu_t)/\rho_e\mu_e$$

are dimensionless parameters; $Re = v_m\rho_{e0}R_N/\mu_{e0}$; $v_m = \sqrt{2h_{e0}}$; $\tau = t/t^*$, $\Theta = T/T_{e0}$ are the dimensionless time and temperature; $t^* = R_N\rho_{1*}c_{1*}/\lambda_{1*}$; R_N, L is the characteristic dimension and thickness of the shell. The subscripts e, e0, and w pertain to parameters on the external boundary of the boundary layer, on the external boundary at the stagnation point, and on the outside surface of the shell, respectively. The subscript 1 denotes characteristics of the solid phase, while the subscripts m and t denote characteristics of molecular and turbulent transfer.

A two-layer model of a turbulent boundary layer was used to describe turbulent flow. The eddy viscosity coefficient in the internal region was found from the Prandtl formula with the Van-Drist-Cebeci damping factor [6]:

$$\mu_t = 0.16\rho y^2\{1 - \exp(-y/A)\}^2 \frac{\partial u}{\partial y}, \tag{1.8}$$
$$A = 26\nu\sqrt{\frac{\rho}{\tau_w}}\,[1 - 11.8\bar{p}]^{1/2},\ \tau_w = \mu\frac{\partial u}{\partial y}\Big|_w,\ \nu = \frac{\mu}{\rho},\ \bar{p} = \frac{\nu u_e}{(\tau_w/\rho)^{3/2}}\frac{du_e}{dx}.$$

In the external region we used the Clauser formula with a correction factor which considered alternation:

$$\mu_t = 0.0168\rho\,[1 + 5.5\,(y/\delta)^6]^{-1}\int_0^\infty (u_e - u)\,dy. \tag{1.9}$$

The boundary between the regions was found from the condition of equality of the coefficients (1.8) and (1.9).

The coefficient of longitudinal alternation Γ for the case of flow about blunt bodies was taken from [7] in the transitional region from the laminar to the turbulent regime. The origin was determined by the point of loss of stability. The coordinate of this point was determined from the condition for the critical value of the Reynolds number:

$$Re^{**} = \frac{u_e\rho_e\delta^{**}}{\mu_e} = 200,\ \delta^{**} = \int_0^\infty \frac{\rho u}{\rho_e u_e}\left(1 - \frac{u}{u_e}\right)dy.$$

In the laminar flow regime, $\Gamma = 0$. In the turbulent regime, $\Gamma = 1$.

The completed calculations and comparison with experimental data [8] showed that the given model of turbulent flow can be used.

We examined flow about spherical bodies and bodies with generatrix equations $y_c = x_c^\alpha$, $\alpha = 0.5$, 0.25, and 0.125 (here, the dimensionless quantities x_c and y_c correspond to a Cartesian coordinate system with its origin at the critical point. The x_c axis is directed along the symmetry axis of solids of revolution.) The data in [9], approximated by means of splines, was used for the pressure distribution on the external boundary of the boundary layer.

In the numerical integration, $Pr_m = 0.72$ and $Pr_t = 1$. The molecular viscosity coefficient was determined either from the Sutherland law or from the power dependence on temperature. The system of boundary-layer equations was integrated numerically by a difference scheme obtained by means of an iterative-interpolational method [10]. The two-dimensional heat-conduction equation in the body was calculated by the decomposition method [11] in combination with the method in [10]. The computational procedure was examined in detail in [3].

In the numerical calculations, the thermophysical characteristics of the material were assumed to be constant, and we varied the following determining parameters of the problem: the Mach number in the incoming flow, $Re = v_m\rho_{e0}R_N/\mu_{e0}$, the initial temperature Θ_{1i}, and the coupling parameter $K = \sqrt{Re}Pr_m\lambda_{e0}/\lambda_{1*}$.

2. We will examine the results of the solution of boundary-value problem (1.1)-(1.7). First, let us examine the case of laminar flow in the boundary layer. Figure 1 shows distributions of dimensionless heat flux $\tilde{q}_w = \lambda_w\partial T/\partial y|_w\sqrt{Re}/\rho_{e0}v_m h_{e0}$ and surface temperature $\Theta_w = T_w/$

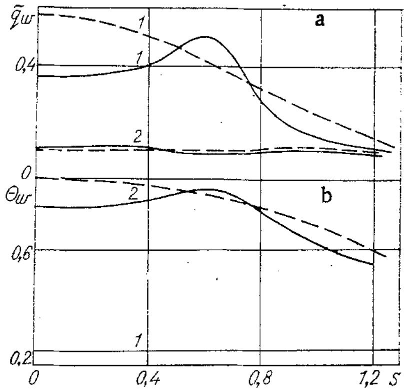

Fig. 1

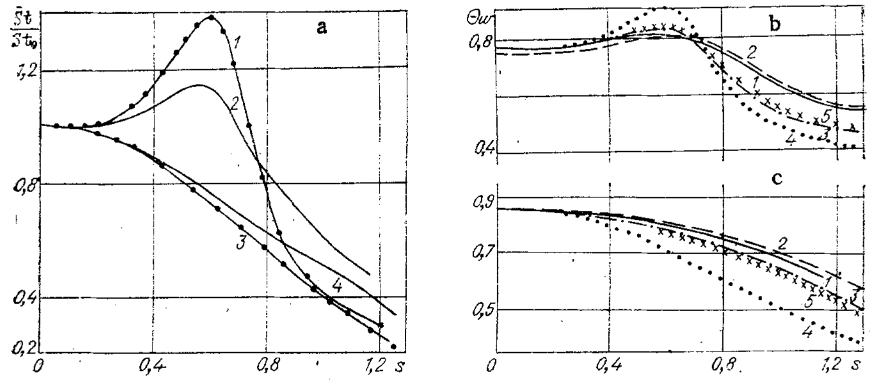

Fig. 2

Te_0 at different moments of time. The calculations were performed for the contour $y_c = x_c^{0.125}$,(solid lines) and a sphere (dashed lines). Curves 1 correspond to $\tau = 0$, while curves 2 correspond to $\tau = 0.08$. Here, $M_\infty = 4$, $\mu/\mu_{e0} = \sqrt{\Theta}$, $T_\infty = 288°K$, $\Theta_{1i} = 0.248$, $K = 3.186$, $L/R_N = 0.1$, $\partial\Theta/\partial y_1|_{y_1 = L/R_N} = 0$. The results were obtained from the solution of a one-dimensional heat-conduction equation because, as will be shown below, heat flow along the longitudinal coordinate s can be ignored for the given determining parameters of the problem. It follows from Fig. 1 that with the generatrix $y_c = x_c^{0.125}$ at the initial moment of time $\tau = 0$ the heat-flux maxima is reached on the lateral surface in the region with the smallest radius of curvature of the contour and the greatest velocity gradient on the external boundary. Over time, this process leads to a maximum surface temperature in the given region and a subsequent decrease in heat flux (curves 2). Results of analysis of the solution in the form of the ratio $St/St_0 = q_w(1 - \Theta_{w0})/[q_{w0}(1 - \Theta_w)]$ for different moments of time (curves 1 and 3 — $\tau = 0$; 2 and r — $\tau = 0.08$) are shown in Fig. 2a (curves 1 and 2 are for the body with $x_c^{0.125}$, while 3 and 4 are for the sphere). The corresponding distribution $\Theta_w(s)$ at $\tau = 0.08$ for $y_c = x_c^{0.125}$ is shown in Fig. 2b, c. The relative heat-flux distribution agrees well with the formulas in [12] and $St/St_0 = q_w/q_{w0}$ for the isothermal surface of the body at $\tau = 0$. The circles in Fig. 2a show data obtained from the formulas in [12] with $\Theta_w = \Theta_{1i}$.

In the general case of an isothermal surface $T_w(s)$, the method of successive approximations [13, 14] can be used to write a formula for the heat-flux ratio

$$\frac{q_w(s)}{q_{w0}} = \sqrt{\frac{u_e\rho_e\mu_e}{2\left.\frac{du_e}{ds}\right|_{s=0}\rho_{e0}\mu_{e0}\alpha}}\left\{\frac{(1-\varphi)B_\infty(0)}{B_\infty(s)}\sqrt{\frac{\delta_g(0)}{\delta_g(s)}} + \right. \tag{2.1}$$
$$\left. + 2\Pr\sqrt{\delta_g(0)\,\delta_g(s)}\,B_\infty(0)\,\alpha\chi\left[1 - \frac{\Phi_1}{2B_\infty(s)}\right]\right\}\frac{(1-\Theta_w)}{(1-\Theta_{w0})},$$

where

$$\varphi = \frac{(1-\Pr_m)}{(1-\Theta_w)}\frac{u_e^2}{v_m^2},\quad \chi = \frac{\partial \ln(1-\Theta_w)}{\partial s},$$

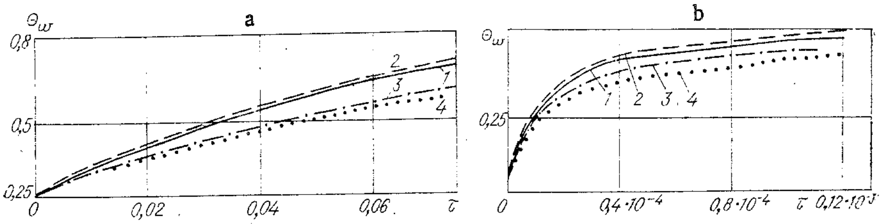

Fig. 3

while the expression for the control function $\delta_g(s)$ has the form

$$\delta_g(s) = \int_0^s \frac{(1-\varphi)\psi}{\Pr B_\infty(s)} \exp\left(\int_0^s \chi \frac{\Phi_1}{B_\infty(s)} ds\right) ds \left[\alpha\psi \exp\left(\int_0^s \chi \frac{\Phi_1}{B_\infty(s)} ds\right)\right]^{-1}, \tag{2.2}$$

$$\psi = \rho_e \mu_e u_e \left(\frac{r_w}{R_N}\right)^2.$$

Here, in accordance with [14], we write the integrals Φ_1 and B_∞ as follows with the sought profiles given in the form of an error integral and the viscosity law $\mu/\mu_{e0} = \sqrt{\Theta}$

$$\Phi_1 = 0.068 + 0.091\left(\frac{\Theta_w(s)}{1-\frac{u_e^2}{v_m^2}}\right)^{1/2},\ B_\infty = 0.068 + 0.057\left(\frac{\Theta_w(s)}{1-\frac{u_e^2}{v_m^2}}\right)^{1/2}.$$

Expanding the functions in the neighborhood of the critical point, we obtain the following, accurate to within the second order:

$$\delta_g(0) = \frac{1}{2\Pr_m B_\infty(0)},\ B_\infty(0) = 0.068 + 0.057\Theta_w^{1/2}. \tag{2.3}$$

The results of numerical integration and analysis of Eq. (2.1) in the case Θ_w = const show that parametric sampling of the value of Θ_w has little effect on the heat-flux ratio [14]. At the same time, it follows from Eq. (2.1) that the second term, connected with the derivative $\partial\Theta_w/\partial s$, may make a substantial contribution to the value of the heat-transfer coefficient in the case of a nonisothermal surface. It was shown in [15] and confirmed by a comparison of theoretical and experimental data that a variable temperature $T_w(s)$ has a significant effect on the Nusselt number in the flow of an incompressible gas about a flat plate.

It follows from a comparison of the curves in Fig. 2a that the ratio St/St_0 obtained for constant and variable surface temperatures may differ appreciably. Here, in accordance with (2.1), St/St_0 decreases on the lateral part of the surface in the region of positive values of $\partial\Theta_w/\partial s$, while it increases for negative values. The use of the coefficient of heat transfer from the gas phase found for an isothermal surface may lead to serious understatement of surface temperature at $\partial\Theta_w/\partial s < 0$ in this case.

The results of the solution in an exact formulation with allowance for coupled heat transfer (curve 1) and the results obtained with the separate formulation are compared in Fig. 2b, c. Here and in Fig. 3, curves 2 correspond to the solution of the heat-conduction equation with a specified heat flux from the gas phase in the form $q_w = [q_w(s)/q_{w0}]q_{w0}$, where $q_w(s)/q_{w0}$ was taken from (2.1). The well-known formulas in [16] were used to calculate heat flux in the neighborhood of the critical point q_{w0}. Here, curves 3 were obtained for the case when the second term was not considered in Eq. (2.1), i.e., with $\chi = 0$. The expression for the control function $\delta_g(s)$ is also simplified in this case.

It follows from comparison of curves $\Theta_w(s)$ with the heat flux assigned with allowance for (2.1) that there is fairly good agreement between the results of the solutions in the exact and separate formulations. If we consider only the history of development of the thermal boundary layer and do not consider the value of the local derivative $\partial\Theta_w/\partial s$, then the surface temperatures are reduced at $\partial\Theta_w/\partial s < 0$. This has a greater effect for the body with $y_c = x_c^{0.125}$, for which there is a significant change in conditions on the external boundary of the boundary layer and, thus, in the surface temperature at $s > 0.6$. The error of Θ_w for the sphere is no greater than 5-6% at $s \leq 1$ and 10% at $s > 1$.

If we use the expression $q_w = (q_w(s)/q_{w0})^0 q_{w0}$ as the heat flux from the gas phase in the separate formulation of the problem – with the relative heat flux $(q_w/q_{w0})^0$ being chosen with an initially isothermal surface temperature – then the error of $\Theta_w(s)$ in such an approach increases significantly (curves 4 in Fig. 3 and Fig. 2b, c). Curves 5 were obtained with the use of the flux $q_w = St(s)(1 - \Theta_w)q_{w0}/[St(0)(1 - \Theta_{w0})]$, where the ratio $St(s)/St(0)$ was taken with Θ_{wi}. These approaches correspond to specification of the coefficient of heat transfer from the gas phase for an isothermal surface.

The effect of nonisothermal temperature $\Theta_w(s)$ on the coefficient of heat transfer from the gas phase can be analyzed by means of the analytical solution (2.1). We will construct the nonisothermality coefficient in the form of the ratio St/St_0 for variable and constant surface temperatures, other conditions being equal:

$$\varkappa = \frac{St/St_0}{(St/St_0)_{is}} = (1-\varphi)\frac{B_\infty(0)}{B_\infty(s)}\sqrt{\frac{\delta_g(0)}{\delta_g(s)}}\left[1+\frac{2\Pr\delta_g(s)B_\infty(s)\alpha\chi}{(1-\varphi)}\left(1-\frac{\Phi_1}{2B_\infty(s)}\right)\right]\left[(1-\varphi)\frac{B_\infty(0)}{B_\infty(s)}\sqrt{\frac{\delta_g(0)}{\delta_g(s)}}\right]^{-1}_{is} \quad (2.4)$$

(the index is corresponds to the characteristics of the isothermal surface). If $\mu \sim T$, then $\Phi_1(s) = \text{const} = 0.159$; $B_\infty(s) = \text{const} = 0.125$, and Eqs. (2.4) and (2.2) can be simplified. Using the assumption $Pr_m = 1$, we obtain

$$\varkappa = \sqrt{\frac{\delta_g(s)_{is}}{\delta_g(s)}}\left[1+2\delta_g(s)B_\infty\alpha\chi\left(1-\frac{\Phi_1}{2B_\infty}\right)\right], \quad (2.5)$$

$$\frac{\delta_g(s)_{is}}{\delta_g(s)} = \frac{\left(\frac{1-\Theta_w}{1-\Theta_{w0}}\right)^{\frac{\Phi_1}{B_\infty}}\int\limits_0^s \rho_e\mu_e u_e\left(\frac{r_w}{R_N}\right)^2 ds}{\int\limits_0^s \rho_e\mu_e u_e\left(\frac{r_w}{R_N}\right)^2\left(\frac{1-\Theta_w}{1-\Theta_{w0}}\right)^{\frac{\Phi_1}{B_\infty}} ds}.$$

Let us examine the case of flow about a sphere when $r_w/R_N = \sin s$. The velocity on the external boundary u_e will be given as $u_e = du_e/ds|_{s=0}s$, while we will use Newton's formula $p_e/p_{e0} = \cos^2 s$ for the distribution of p_e. Considering the character of the distribution $q_w(s)$ about the circumference of the sphere, we specify $\Theta_w(s)$ in the form $(1 - \Theta_w)/(1 - \Theta_{w0}) = (1 + As^2)^{B_\infty/\Phi_1}$, where A is a positive constant coefficient. At $A = 0$, we have $\Theta_w(s) = \Theta_{w0} = \text{const}$. Then from (2.5),

$$\frac{\delta_g(s)_{is}}{\delta_g(s)} = \frac{1+As^2}{1+A\int\limits_0^s s^3\cos^2 s\sin^2 s\,ds\left(\int\limits_0^s s\cos^2 s\sin^2 s\,ds\right)^{-1}}, \quad (2.6)$$

$$\frac{\int\limits_0^s s^3\cos^2 s\sin^2 s\,ds}{\int\limits_0^s s\cos^2 s\sin^2 s\,ds} = \frac{s^4 - s^3\sin 4s - 0{,}75\,s^2\cos 4s + (3/8)\,s\sin 4s + (3/32)\cos 4s - 3/32}{2s^2 - s\sin 4s - 0{,}25\cos 4s + 0{,}25}. \quad (2.7)$$

Considering that $2\delta_g(s)B_\infty = \delta_g(s)/\delta_g(s)_{is}$, $\chi = \dfrac{B_\infty 2As}{\Phi_1(1+As^2)}$, $\alpha = (2s^2 - s\sin 4s - 0.2s\cos 4s + 0.25)/(16s\sin^2 s\cos^2 s)$, it is easy to find $\varkappa$. We will determine A from the condition $\Theta_w(s_*) = \Theta_*$ on the given ray s_*, when $A = \left[((1-\Theta_*)/(1-\Theta_{w0}))^{\frac{\Phi_1}{B_\infty}} - 1\right]\Big/ s_*^2$. At large values of Θ_{w0}, $A > 1$; for example, it follows from Fig. 2c that $\Theta_{w0} = 0.86$, $\Theta_* = 0.6$, $s_* = 1.2$, so that $A = 1.95$. From here, with $s = 1.3$, $\sqrt{\delta_g(s)_{is}/\delta_g(s)} = 1.295$, $\varkappa = 2.17$ from the solution of (2.5)-(2.7). At small values of Θ_w, $A = 0.05$-0.15; thus, for $\Theta_{w0} = 0.19$, $s = 1.3$, $A = 0.113$, so that $\sqrt{\delta_g(s)_{is}/\delta_g(s)} = 1.045$, $\varkappa = 1.27$.

The above analysis confirms the conclusions regarding the need to allow for surface nonisothermality in the expression for St/St_0 in sections far from the critical point within a broad range of values of the temperature factor. This is corroborated by the theoretical data in Fig. 3a, b, where the dynamics of the change in surface temperature with time at $s = 0.86$ is shown for the body with $y_c = x_c^{0.125}$ for the exact and separate formulations of the

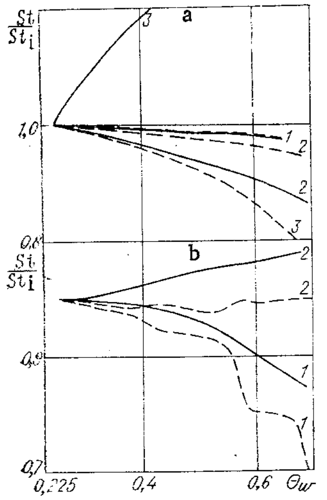

Fig. 4

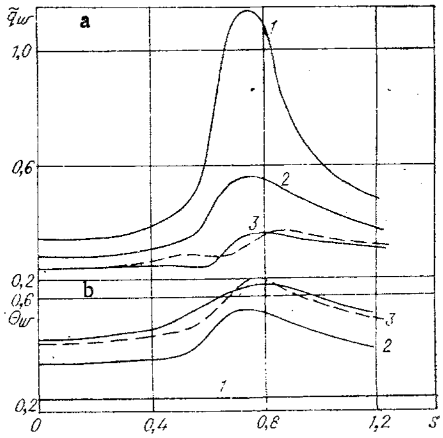

Fig. 5

problem. Figure 3a corresponds to the calculation shown in Fig. 1, while Fig. 3b gives results of calculations of flow about the body with $M_\infty = 10$ and other determining parameters being identical. In this case, with $T_{wi} = 300$ K, $\Theta_{1i} = 0.0496$, and it is evident that the difference in $T_w(\tau)$ also becomes significant over time in the section $s = 0.86$.

Calculation of the boundary-value problem (1.1)-(1.7) showed that the temperature across the shell equalizes for adiabatic conditions on the inside wall of the shell at large values of τ, and $\Theta_w(s)$ attains the radiative equilibrium temperature $\Theta_{wr}(s)$. The latter is also determined independently of problem (1.1)-(1.5) with an energy conservation balance condition

$$q_w(0, s)\sqrt{\mathrm{Re}}\,\mathrm{Pr_m}\frac{\lambda_{e0}}{\lambda_{1*}} = \pi_\sigma\Theta_w^4. \tag{2.8}$$

Here, for $\varepsilon = 0.7$, $M_\infty = 4$, $T_{e_0} = 1210$ K the parameter π_σ is small and the distribution of Θ_{wr} about the circumference of the body is somewhat lower than the value of the adiabatic surface temperature, which can be evaluated beforehand [17]. With an increase in M_∞, the stagnation temperature T_{e_0} increases. This in turn leads to an increase in π_σ and a decrease in Θ_{wr}. Meanwhile, the value of Θ_{wr} changes much more drastically about the circumference of the body.

Figure 4a shows the results of analysis of the solution of the coupled problem in Fig. 1c in the form of the ratio $St/St_i = q_w(s^*)[1 - \Theta_{wi}(s^*)]/q_{wi}(s^*)(1 - \Theta_w(s^*))]$, where St_i corresponds to the initial isothermal surface temperature. The data are shown for different values of the coordinate s^* about the circumference of the body. The dashed curves correspond to values of St/St_i found by integration of the boundary-layer equations with different isothermal values of the wall temperature. Curves 1-3 were constructed with $s = 0$, 0.6, and 0.86 for the body with $y_c = x_c^{0.125}$.

As might be expected, the results of calculations with both formulations agree near the stagnation point, but they may differ appreciably on the lateral surface (curves 3). For this reason, as indicated above, the use of the heat-transfer law obtained for an isothermal wall will lead to significant errors in the determination of Θ_w on the lateral surface of the given bodies.

Figure 5 shows the behavior of dimensionless heat flux $\tilde{q}_w(s, \tau)$ and surface temperature at different moments of time in the presence of laminar, transitional, and turbulent regions of boundary-layer flow. Here $M_\infty = 4$, $T_\infty = 288$°K, $\Theta_{1i} = 0.248$, $K = 3.186$, $L/R_N = 0.1$, $\mu/\mu_{e_0} = \Theta^{3/2}(1 + c)/(\Theta + c)$, $\partial\Theta/\partial y_1|_{y_1=L/R_N} = 0$, $\mathrm{Re} = 5.7\cdot 10^6$, and we examined flow about a body with a contour described by the equation $y_c = x_c^{0.125}$. Curves 1-3 correspond to $\tau = 0$, 0.01, and 0.02. The solid lines were obtained from the solution of the boundary-value problem with the use of two-dimensional energy equation (1.3), while the dashed lines were obtained for $\tau = 0.02$ with the use of a one-dimensional equation, when heat flow along the longitudinal coordinate s is ignored. It should be noted that the conditions of these calculations (sufficiently large thermal conductivity in the body, large longitudinal temperature gradient on the surface due to turbulent boundary-layer flow) maximize the difference of $\Theta_w(s)$ (to 10%). In the case of low thermal conductivities in the body or with laminar flow in the boundary layer, heat flow along the longitudinal coordinate can be ignored.

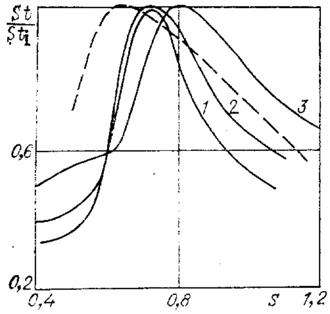

Fig. 6

The conservativeness of the ratio St/St* was shown in [17, 18] for spherical blunting, where $St^* = q_w^*[\rho_\infty v_\infty c_p(T_{e0} - T_w^*)]$ corresponds to the maximum heat flux q_w^* for an isothermal surface in a broad range of determining parameters of the problem. It is interesting to analyze the behavior of this quantity when the body is heated. The results of the solution shown in Fig. 5 were analyzed in the form St/St*(s) for the same moments of time and are shown in Fig. 6, where 1-3 correspond to τ = 0, 0.01, and 0.02. The dashed line corresponds to flow about a sphere with allowance for the transitional zone at $\Theta_w = \Theta_{1i} = 0.248$ and the determining parameters in Fig. 5. Good agreement is obtained with the formula in [18] obtained using the effective-length method [19] for St/St* in the case Θ_w = const with the use of the model of point transition from laminar to turbulent boundary-layer flow.

It can be seen from Fig. 6 that the ratio St/St* changes little over time for different behaviors of surface temperature about the circumference of the body. Here, the use of St/St* found for an isothermal surface as the coefficient of heat transfer from the gas phase with the separate method of solution of the problem will lead to a significant reduction in the temperature of the lateral surface, as in the case of laminar boundary-layer flow.

This conclusion also follows from Fig. 4b, which compares results of the solution in the coupled formulation from the calculated data in Fig. 5 (solid curves) with data from numerical integration of the system of equations with different isothermal values of surface temperature (dashed lines). Here, the lines characterizing the dependence of St/St_i on Θ_w for turbulent boundary-layer flow are shown for two values of s about the circumference (1 and 2 correspond to s = 0.86 and 1.23).

Results of numerical integration of boundary-value problem (1.1)-(1.7) were compared with results obtained by formulas in the effective-length method [19] for heat flux with heating of bodies of different form, these formulas having been obtained for the general case of a nonisothermal surface:

$$q_w = 0.0296\,\mathrm{Pr}_m^{-0,57} k_1 \rho_w^{0,8} u_e^{0,8} \mu_w^{0,2} x_{ef}^{-0,2} c_p (T_r - T_w),$$

$$k_1 = \left(\frac{T_w}{T_r}\right)^{[0,4+0,2\exp(-0,89\omega)]} (1 + 0.89\omega)^{0,11},$$

$$\omega = u_e^2/2h_e,\ T_r = T_{e0}\left(\frac{1+0,89\omega}{1+\omega}\right),$$

$$x_{ef} = \int_0^s \rho_w \mu_w^{0,25} \left(\frac{k_1 r_w}{\mathrm{Pr}_m}\right)^{1,25} (T_r - T_w)^2 ds \Big/ \left\{\rho_w \mu_w^{0,25} \left(\frac{k_1 r_w}{\mathrm{Pr}_m}\right)^{1,25} (T_r - T_w)^2\right\}.$$

A point transition from laminar to turbulent flow was specified for the separate formulation. Here the calculations agreed on surface temperature to within about 8% in the region of developed turbulent flow for the sphere. For the body with $y_c = x_c^{0.125}$ and separate formulation of the problem, the reduction in surface temperature reaches 15% at s > 0.8 and τ = 0.02.

LITERATURE CITED

1. A. V. Lykov, Heat and Mass Transfer (Handbook) [in Russian] Énergiya, Moscow (1972).
2. V. I. Zinchenko and E. G. Trofimchuk, "Solution of nonsimilar problems of the theory of laminar boundary-layer flow with allowance for coupled heat transfer," Izv. Akad. Nauk SSSR, Mekh. Zhidk. Gaza, No. 4 (1977).

3. V. I. Zinchenko and E. N. Putyatina, "Heat and mass transfer in flow about bodies of different form with allowance for injection," Inzh.-Fiz. Zh., 45, No. 1 (1983).
4. P. R. Chapman and H. W. Rubbesin, "Temperature and velocity profiles in the compressible laminar boundary layer with arbitrary distribution of surface temperature," J. Aeron. Sci., 16, No. 9 (1949).
5. A. Sh. Dorfman, Heat Transfer in Flow about Nonisothermal Bodies [in Russian], Mashinostroenie, Moscow (1982).
6. Tuncer Cebeci, "Behavior of turbulent flow near a porous wall with pressure gradient," AIAA J., 8, No. 12 (1970).
7. K. K. Chen and N. A. Thyson, "Extension of Emmons spot theory to flows on blunt bodies," AIAA J., 9, No. 5 (1971).
8. R. H. Feldhuhn, "Heat transfer from a turbulent boundary layer on a porous hemisphere," AIAA Paper No. 119 (1976).
9. L. N. Lyubimov and V. V. Rusanov, Gas Flow about Blunt Bodies [in Russian], Vol. 2, Nauka, Moscow (1970).
10. A. M. Grishin and V. N. Bertsun, "Iterative—interpolational method and the theory of splines," Dokl. Akad. Nauk SSSR, 214, No. 4 (1974).
11. N. N. Yanenko, Method of Fractional Steps for Solving Multidimensional Problems of Mathematical Physics [in Russian], Nauka, Novosibirsk (1967).
12. Camp, Rouse, and Detra, "Laminar heat exchange between blunt bodies and a flow of dissociated air," in: Gasdynamics and Heat Transfer in the Presence of Chemical Reactions [Russian translation], IL, Moscow (1962).
13. G. A. Tirskii, "Method of successive approximations for integrating equations of a laminar multiple-component boundary layer with chemical reactions, including an ionization reaction," Otchet Inst. Mekh. Mosk. Gos. Univ., No. 1016 (1969).
14. I. G. Brykina, É. A. Gershbein, and S. V. Peigin, "Laminar three-dimensional boundary-layer on a permeable surface near a symmetry plane," Izv. Akad. Nauk SSSR, Mekh. Zhidk. Gaza, No. 5 (1980).
15. A. Zhukauskas and N. Zhyugzhda, Heat Transfer in Laminar Flow [in Russian], Mintis, Vilnius (1969).
16. D. Fay and F. Riddel, "Theoretical analysis of heat transfer at a forward critical point washed by dissociated air," in: Gasdynamics and Heat Transfer in the Presence of Chemical Reactions [Russian translation], IL, Moscow (1962).
17. Yu. V. Lapin, Turbulent Boundary Layer in Supersonic Gas Flows [in Russian], Nauka, Moscow (1982).
18. B. A. Zemlyanskii and G. N. Stepanov, "Calculation of heat transfer in three-dimensional hypersonic flow of air about thin blunt cones," Izv. Akad. Nauk SSSR, Mekh. Zhidk. Gaza, No. 5 (1981).
19. V. S. Avduevskii, B. M. Galitseiskii, G. A. Glebov, et al., Principles of Heat Transfer in Aviation and Rocket-Space Technology [in Russian], Mashinostroenie, Moscow (1975).